PHYSICAL REVIEW A VOLUME 27, NUMBER 1 JANUARY 1983

Light propagation and light scattering in cholesteric liquid crystals

Mark A. Peterson
Department of Physics, George Mason University, Fairfax, Virginia 22030
(Received 17 December 1981)

The exact solution to Maxwell's equations in a cholesteric planar texture is described and an algorithm for computing it is given. This algorithm makes use of a matrix continued fraction which converges so rapidly that the solution is, for practical purposes, in closed form. The solutions thus found can be used to describe scattering from dielectric inhomogeneities in a cholesteric in Born approximation, taking exact account of the cholesteric medium in which the scattering takes place. The general expression for the S matrix in the Born approximation is given. The consequences for scattering from slowly varying order-parameter fluctuations are worked out in detail and several features are noted which depend in an essential way on the form of the exact cholesteric modes. These features include: (1) the scattered amplitude goes to zero in the forward direction, (2) there is a kind of anomalous diffraction for wavelengths near the pitch length, and (3) the scattered light may show complex spatial structure, even if the scatterer is essentially structureless, due to a kind of spatial beating of the cholesteric modes.

INTRODUCTION

It is well known that cholesteric liquid crystals exhibit striking and unique optical properties. Our understanding of these properties is due to many authors, in particular Oseen,[1] de Vries,[2] D. Taupin,[3] Berreman and Scheffer,[4] Dreher and Meier,[5] and V. A. Belyakov and V. D. Dmitrienko.[6] It appears that no previous investigation, however, has given the exact, general off-axis solution to Maxwell's equations in a cholesteric planar texture. In Taupin's method[3] it must be found as the null vector of an infinite matrix. The methods of Berreman and Scheffer[4] and of Dreher and Meier[5] require numerical integration of systems of ordinary differential equations. The solution of Belyakov and Dmitrienko,[6] although analytic and in closed form, is only approximate ("two-wave approximation"), and one has no *a priori* estimate of how good this approximation is. These authors have pointed out how it must be modified near higher-order reflections.[7] We will see, however, that it is incapable of describing light scattering from order-parameter fluctuations at any angle, as this phenomenon depends in a delicate way on components the two-wave approximation ignores.

In Sec. I of this paper we give the exact solution to Maxwell's equations in a cholesteric in what is, for practical purposes, closed form—it is actually a matrix continued fraction. The dispersion relation must still be solved numerically, however. We illustrate the method by rederiving the known solution for propagation along the helix axis. In Sec. II, we make use of these exact solutions to describe light scattering in a cholesteric in Born approximation, taking the effect of the medium into account. We show by means of an example (scattering from order-parameter fluctuations) that this careful approach is quite necessary in treating scattering from a cholesteric. Impressions based upon thinking of the light as a plane wave are misleading. Light scattering from order-parameter fluctuations is a subtle process, involving in an essential way no fewer than *four* Fourier components of each propagating mode. Spatial structure in the scattered light may be due largely to the form of the modes themselves and not, as intuition would suggest, to structure in the scatterer. This effect, although it is a straightforward consequence of the Born approximation, appears to be novel in the sense that it has no familiar analog. It is a little like the case of scattering of electromagnetic radiation by a dielectric sphere: the sphere itself is simple, but the scattering pattern may show all the complexity of the electromagnetic modes of the sphere. In scattering from cholesterics there is an unexpected dimension of complexity, in that the scattering pattern may depend nontrivially on the azimuthal angle as well, even for an azimuthally symmetric scatterer.

I. LIGHT PROPAGATION

A. General theory

Maxwell's equations in a cholesteric planar texture become

$$-\vec{\nabla}\times(\vec{\nabla}\times\vec{\mathrm{E}})+\frac{\omega^2}{c^2}\overleftrightarrow{\epsilon}\vec{\mathrm{E}}=0\ , \tag{1}$$

where $\overleftrightarrow{\epsilon}$ is the dielectric tensor described below, $\vec{\mathrm{E}}(\vec{r})e^{-i\omega t}$ is the electric field, and c is the speed of light in vacuum. We assume $\overleftrightarrow{\epsilon}$ can be represented as

$$\overleftrightarrow{\epsilon}=\epsilon_\perp I+(\epsilon_{||}-\epsilon_\perp)\hat{n}\hat{n}+(\epsilon_z-\epsilon_\perp)\hat{z}\hat{z}\ , \tag{2}$$

where

$$\hat{n}=\hat{x}\cos qz+\hat{y}\sin qz \tag{3}$$

is the director. Here $\epsilon_\perp$, $\epsilon_{||}$, and ϵ_z are the principal dielectric constants and $q\hat{z}$ is the wave vector of the spatially periodic cholesteric structure.

Although it is believed that most cholesterics are locally uniaxial ($\epsilon_\perp=\epsilon_z$), this assumption does not notably simplify the formalism which follows, so we consider only the general case. The experimental basis for the belief that cholesterics are locally uniaxial is in fact not very extensive. It is essentially one experiment on one material.[4]

We adopt circular basis vectors $\hat{e}_m$ related to Cartesian unit vectors by

$$\begin{aligned}\hat{e}_{\pm1}&=\frac{1}{\sqrt{2}}(\hat{x}\pm i\hat{y})\ ,\\ \hat{e}_0&=\hat{z}\ .\end{aligned} \tag{4}$$

With respect to this basis, the electric field is

$$\vec{\mathrm{E}}=\sum_m E_m\hat{e}_{-m}\ , \tag{5}$$

where

$$\begin{aligned}E_{\pm1}&=\frac{1}{\sqrt{2}}(E_x\pm iE_y)\ ,\\ E_0&=E_z\ .\end{aligned} \tag{6}$$

Also,

$$\hat{n}=\frac{1}{\sqrt{2}}(e^{iqz}\hat{e}_{-1}+e^{-iqz}\hat{e}_1)\ . \tag{7}$$

Hence

$$\overleftrightarrow{\epsilon}=\begin{pmatrix}\epsilon_0 & 0 & \Delta e^{2iqz}\\ 0 & \epsilon_z & 0\\ \Delta e^{-2iqz} & 0 & \epsilon_0\end{pmatrix}\ , \tag{8}$$

where

$$\epsilon_0=\tfrac{1}{2}(\epsilon_{||}+\epsilon_\perp)$$

and

$$\Delta=\tfrac{1}{2}(\epsilon_{||}-\epsilon_\perp)\ .$$

The rows and columns of the matrix ϵ are labeled by 1, 0, -1, and the matrix acts on the components E_m arranged in a column. As we show by explicit construction, Eq. (1) with $\overleftrightarrow{\epsilon}$ given by (8), has solutions of the form

$$[\vec{\mathrm{E}}(\vec{r})]_m=\sum_{n\ \text{odd}}E_{nm}e^{i(p+nq)z}e^{ikr\cos(\theta-\varphi)}e^{i(m-n)\varphi} \tag{9}$$

where the E_{nm} are constants. Let us write $\vec{\mathrm{E}}_n$ for the vector whose components are E_{nm}. Here (r,θ,z) are cylindrical coordinates in space. Also (k,φ,p) are corresponding cylindrical coordinates in momentum space which serve to label this solution, just as the wave-vector labels a plane-wave solution in a homogeneous medium. In particular, k is the momentum transverse to the helix axis, and φ is the azimuthal direction in which the solution propagates.

Substitution of this form into Eq. (1) gives an infinite system of coupled algebraic equations for the E_n,

$$\Delta\delta(-1,1)\vec{\mathrm{E}}_{n+2}+A_n\vec{\mathrm{E}}_n+\Delta\delta(1,-1)\vec{\mathrm{E}}_{n-2}=0\ , \tag{10}$$

where $\delta(i,j)$ is the 3×3 matrix

$$[\delta(i,j)]_{kl}=\delta_{ik}\delta_{jl}\ ,$$

and A_n is the 3×3 matrix with

$$\begin{aligned}(A_n)_{11}=(A_n)_{-1,-1}&=\frac{\omega^2}{c^2}\epsilon_0-\frac{k^2}{2}-(p+nq)^2\\ &\overset{\text{def}}{=}L_n\ ,\\ (A_n)_{00}&=\frac{\omega^2}{c^2}\epsilon_z-k^2\overset{\text{def}}{=}K\ ,\\ (A_n)_{10}=(A_n)_{0,-1}&=(A_n)_{01}=(A_n)_{-1,0}\\ &=\frac{k(p+nq)}{\sqrt{2}}\overset{\text{def}}{=}J_n\ ,\\ (A_n)_{1,-1}=(A_n)_{-1,1}&=\frac{k^2}{2}\ .\end{aligned} \tag{11}$$

Let us seek a solution of Eq. (10) in the form

$$\vec{\mathrm{E}}_n=-\Delta B_n\delta(1,-1)\vec{\mathrm{E}}_{n-2}\ , \tag{12}$$

where B_n is a 3×3 matrix to be determined. Substitution of Eq. (12) into Eq. (10) shows that Eq. (10) is satisfied if we take B_n to be

$$B_n=[A_n-\Delta^2\delta(-1,1)B_{n+2}\delta(1,-1)]^{-1}\ . \tag{13}$$

Similarly we obtain a solution to Eq. (10) by taking

$$\vec{E}_n = -\Delta C_n \delta(-1,1)\vec{E}_{n+2}\,, \tag{14}$$

where

$$C_n = [A_n - \Delta^2 \delta(1,-1) C_{n-2} \delta(-1,1)]^{-1}\,. \tag{15}$$

Iterating the recursion relations (13) and (15) for B_n and C_n, one obtains a nested sequence of matrix inverses, the matrix analog of a continued fraction. (Just as in the case of ordinary continued fractions, the nonexistence of an inverse rather simplifies matters than complicates them. This is discussed later on.)

In fact, B_n depends upon its predecessor B_{n+2} only through the (1,1) element, and similarly C_n depends upon C_{n-2} only through the $(-1,-1)$ element. Hence we define

$$\begin{aligned} \beta_n &= (B_n)_{11}\,, \\ \gamma_n &= (C_n)_{-1,-1}\,. \end{aligned} \tag{16}$$

Then the recursion relations become

$$\begin{aligned} \beta_n &= (W_n \beta_{n+2} + X_n)/(Y_n \beta_{n+2} + Z_n)\,, \\ \gamma_n &= (W_n \gamma_{n-2} + X_n)/(Y_n \gamma_{n-2} + Z_n)\,, \end{aligned} \tag{17}$$

where

$$\begin{aligned} W_n &= -\Delta^2 K\,, \\ X_n &= KL_n - J_n^2\,, \\ Y_n &= -\Delta^2 X_n\,, \\ Z_n &= KL_n^2 + k^2 J_n^2 - \frac{k^4}{4} K - 2L_n J_n^2\,. \end{aligned} \tag{18}$$

One can write these recursion relations more simply by introducing the matrix

$$S_n = \begin{bmatrix} W_n & X_n \\ Y_n & Z_n \end{bmatrix}, \tag{19}$$

and vectors $(\beta_n,1)$ understood as homogeneous coordinates in a projective space [i.e., $(\beta_n,1)$ and $(\alpha\beta_n,\alpha)$ are equivalent for any number $\alpha \neq 0$, and both represent the number β_n]. Then (17) becomes

$$\begin{aligned} \begin{bmatrix} \beta_n \\ 1 \end{bmatrix} &= S_n \begin{bmatrix} \beta_{n+2} \\ 1 \end{bmatrix}, \\ \begin{bmatrix} \gamma_n \\ 1 \end{bmatrix} &= S_n \begin{bmatrix} \gamma_{n-2} \\ 1 \end{bmatrix}. \end{aligned} \tag{20}$$

Iterating the recursion relation is then simply accomplished by matrix multiplication,

$$\begin{bmatrix} \beta_n \\ 1 \end{bmatrix} = S_n S_{n+2} \cdots S_{n+2j} \begin{bmatrix} \beta_{n+2j+2} \\ 1 \end{bmatrix}. \tag{21}$$

The right-hand side of Eq. (21) converges rapidly as $j \to \infty$ and is insensitive to the vector one starts with. Two effects contribute to this rapid convergence. In the first place, S_n for large n takes any vector to (essentially) $\binom{0}{1}$ so that the starting vector is not important. Second, for $k = 0$ the convergence is exact after a single step—the effect of more iterations is to build in the k dependence for nonzero k. For physical k, proximity to the singular case $k = 0$ seems to guarantee rapid convergence. In practice there is not much to be gained from making more than three or four iterations to find β_n. Hence we have solutions for β_n and γ_n,

$$\begin{aligned} \begin{bmatrix} \beta_n \\ 1 \end{bmatrix} &= \lim_{j\to\infty} S_n S_{n+2} \cdots S_{n+2j} \begin{bmatrix} 0 \\ 1 \end{bmatrix}, \\ \begin{bmatrix} \gamma_n \\ 1 \end{bmatrix} &= \lim_{j\to\infty} S_n S_{n-2} \cdots S_{n-2j} \begin{bmatrix} 0 \\ 1 \end{bmatrix}, \end{aligned} \tag{22}$$

where it is understood that the limit $j \to \infty$ is essentially attained at $j \cong 3$.

Knowing β_n and γ_n, we construct B_n and C_n from (13) and (15). This requires a matrix inverse which, in principle, might not exist, but which in practice is never a problem. The singular matrices form a set of measure zero and one does not run into them for generic choices of parameters. The one special case where one does, for physical reasons, encounter a singular B_n is for $k = 0$ (normal incidence). The phenomenon presents no difficulty there, but merely causes the series representation of the solution in Eq. (9) to terminate after a finite number of terms, as we show in part B of this section. Indeed, as we pointed out above, it seems to be proximity to this singular case which makes the convergence so rapid for general k.

Now if we choose a vector $\vec{E}_N$ we can construct from it $\vec{E}_{N+2}, \vec{E}_{N+4}, \cdots$ using Eq. (12) and $\vec{E}_{N-2}, \vec{E}_{N-4}, \cdots$ using Eq. (14). The process is numerically stable. The set $\{\vec{E}_n\}$ so obtained solves Eq. (10) at every stage except N, where we must still require

$$[A_N - \Delta^2 \beta_{N+2} \delta(-1,-1) - \Delta^2 \gamma_{N-2} \delta(1,1)]\vec{E}_N = 0\,, \tag{23}$$

and hence

$$\det[A_N - \Delta^2 \beta_{N+2} \delta(-1,-1) - \Delta^2 \gamma_{N-2} \delta(1,1)] = 0\,. \tag{24}$$

Equation (24) is the dispersion relation. For fixed k it can be met by choosing p appropriately. The dispersion relation can be written more compactly

as a quadratic form

$$(\gamma_{N-2},1)Q_N\begin{bmatrix}\beta_{N+2}\\1\end{bmatrix}, \tag{25}$$

where Q_N is the matrix of the quadratic form. It turns out that

$$Q_N = MS_N ,$$

where

$$M=\begin{bmatrix}-\Delta^2 & 0\\ 0 & 1\end{bmatrix} \tag{26}$$

and S_N is given by Eq. (19). Using Eq. (22), we can express the dispersion relation as

$$0=(0,1)\cdots S_{N-4}^T S_{N-2}^T \times MS_N S_{N+2}S_{N+4}\cdots\begin{bmatrix}0\\1\end{bmatrix}. \tag{27}$$

Then, since

$$S_n^T M = MS_n , \tag{28}$$

the matrix M in Eq. (27) can be moved to the left like a "zipper," undoing the transposes and leaving the dispersion relation in the symmetrical form

$$0=(0,1)\cdots S_{N-4}S_{N-2}S_N \times S_{N+2}S_{N+4}\cdots\begin{bmatrix}0\\1\end{bmatrix}. \tag{29}$$

Taking a finite number of S_n's in Eq. (29) yields an approximation to the dispersion relation which is a polynomial equation in p.

Another form of the dispersion relation, from Eq. (27) and (22), is

$$\Delta^2\beta_N\gamma_{N-2}=1 . \tag{30}$$

Also, from Eq. (18) we have

$$S_n(p)=S_{-n}(-p) , \tag{31}$$

so, from (22)

$$\gamma_{-n}(-p)=\beta_n(p) . \tag{32}$$

From Eq. (29) we know the form of the dispersion relation (30) is independent of N, so taking $N=1$ in (30) we can write it as

$$\Delta^2\beta_1(p)\beta_1(-p)=1 , \tag{33}$$

which is invariant under $p\rightarrow -p$. Symmetrically chosen polynomial approximations to Eq. (29) or rational approximations to Eq. (30) build in this exact symmetry of the problem and are actually equations in p^2. Real solutions with $p^2<0$ then describe evanscent waves (associated with the reflection bands), and solutions with $p^2>0$ describe traveling waves. (This remark about real and imaginary p assumes $\epsilon_\perp$, $\epsilon_{||}$, ϵ_z real. If the dielectric constants are complex, one still has the symmetry $p\rightarrow -p$, and the sign of the imaginary part is related to the sign of the group velocity so as to preserve causality: the wave dies off in the same direction as wave packets propagate.)

Since one can always translate p into the first Brillouin zone $|\mathrm{Re}p|\leq q$ by relabeling the $\vec{E}_n$'s, only the two smallest roots for p^2 are required. The effect of higher-order polynomial approximations to the dispersion relation is mainly to build in the redundant roots required by translation symmetry, and hardly at all to refine the lower roots, which converge rapidly to their exact values.

This convergence is illustrated in Table I. The parameters are chosen so that none is particularly small. The rapidity of the convergence is faster than one would expect intuitively from, say, a power series in k and Δ. It seems to be true, although we have not been able to supply a proof, that the convergence is as good as this for all parameter values of physical interest. In particular, nothing exceptional happens in the reflection bands (except that p becomes complex).

Let us summarize how one constructs the solution labeled by $[k,\varphi,p(k)]$.

(1) Solve the dispersion relation in the form (24), (29), (30), or (33) for $p(k)$.

(2) Check condition (24) to see which root $p(k)$ has been found [$p(k)$ translated by any integer multiple of $2q$ is another root of (29), (30), or (33) corresponding to a different choice for N in Eq. (24)].

TABLE I. Roots p of the dispersion relation (29), approximated as a polynomial in p^2 of degree $2j$, for $k=0.4$, $q=0.5$, and $\Delta=0.315$. Note rapid convergence of roots horizontally and appearance of redundant roots vertically. For each root p in the table, $-p$ is also a root.

$j=1$	$j=2$	$j=3$	$j=4$
			−1.585 054 2
		−0.585 054 2	−0.584 757 6
	0.414 945 5	0.415 242 4	0.415 242 4
1.408 904	1.415 270 7	1.415 242 4	1.415 242 4
0.337 590	0.334 793 7	0.334 806 8	0.334 806 8
	1.335 149 3	1.334 804 7	1.334 806 8
		2.335 149 3	2.334 804 7
			3.335 149 3

(3) $\vec{E}_N$ is given by Eq. (23).

(4) $\vec{E}_{N+2}$, $\vec{E}_{N+4}$, . . ., and $\vec{E}_{N-2}$, $\vec{E}_{N-4}$, . . ., are given by Eqs. (12) and (14).

These constants completely specify the solution in the form of Eq. (9). Accuracy of the solution can be simply checked by substitution into Eq. (10).

The advantages of this solution over other published numerical methods[3-5] are several.

(i) Although it is long to describe, it requires very few steps to compute. Step (3) above requires the evaluation of two continued fractions and three 2×2 determinants. Each component of the field in step (4) above requires the evaluation of one continued fraction and the inversion of one 3×3 matrix. By contracts, the most frequently used method for this problem, that of propagation matrices,[4] requires the multiplication of typically hundreds of 4×4 matrices in a numerical integration, with the danger of accumulating error.

(ii) Our solution can be simply checked by substitution into the (algebraic) equation it is supposed to satisfy. A numerical solution to a differential equation is not so easily checked.

(iii) Our solution, in the form of Eq. (9), is not particularized to a specific material geometry, but is rather the basis in which such specific solutions are most naturally expressed. Thus one can easily derive algebraic expressions involving the E_{nm}'s for reflection and transmission coefficients at a plane dielectric interface by imposing the usual boundary conditions. The Fabry-Perot problem of multiple reflections to all orders is scarcely more difficult. In contrast, a solution found by numerical integration is tied to particular initial conditions, sample thickness, etc. Such solutions, while they may treat particular experimental situations, are not convenient for discussing general phenomena, such as scattering.

On the other hand, our method does not easily generalize to the case of the smectic C^* phase, while the propagation matrix method does.[8]

The φ dependence of the solution is competely explicit in Eq. (9), since $p(k)$ and the E_{nm}'s are independent of φ. Perhaps the clearest way to think of it, though, is to associate the last φ-dependent factor in Eq. (9) with the constants E_{nm}. Then we could say that for every solution with constants E_{nm} there is another solution, rotated through the azimuthal angle φ, with constants $E_{nm}e^{i(m-n)\varphi}$, as if E_{nm} transformed according to the $m-n$ representation of $O(2)$. The solution as a whole transforms according to a *reducible* representation of $O(2)$, which is only to be expected, since the original problem does not possess azimuthal symmetry.

One can describe behavior under the reflection $z\rightarrow -z$ similarly. For every solution with constants p and E_{nm}, there is a reflected solution with constants $-p$ and $(-1)^m E_{-n,-m}$. Again the representation is in general reducible, since the problem does not have reflection symmetry. Under parity we have $p\rightarrow -p$ and $E_{nm}\rightarrow E_{-n,-m}$.

With the absence of familiar symmetries comes the absence of familiar selection rules, with consequences for scattering theory.

B. Example: Propagation along the axis

We illustrate the method in the slightly singular case $k=0$, propagation along the helix axis, which has been treated by many authors.[9]

In this case S_n is singular, so that (22) converges in a single step to

$$\beta_n=\gamma_n=1/L_n\ . \tag{34}$$

The dispersion relation, from Eq. (24) with $N=1$, is then

$$L_{-1}L_1=\Delta^2 \tag{35}$$

with roots $p_\pm$ given by

$$p_\pm^2=1+q^2\pm(4q^2+\Delta^2)^{1/2}\ , \tag{36}$$

where we have chosen units of length such that $(\omega^2/c^2)\epsilon_0=1$. Both roots lead in Eq. (23) to $\vec{E}_1^{(\pm)}=(1,0,0)$. Use of Eq. (12) shows $\vec{E}_N^{(\pm)}=0$ for $N>1$. Use of Eq. (14) shows $\vec{E}_{-1}^{(\pm)}=[0,0,-\Delta/L_{-1}(p_\pm)]$ and $\vec{E}_N^{(\pm)}=0$ for $N<-1$. Hence, we have the well known (unnormalized) solutions for normal incidence

$$\vec{E}^{(\pm)}(\vec{r})=\begin{bmatrix}0\\0\\-\Delta/L_{-1}\end{bmatrix}e^{i(p_\pm-q)z}+\begin{bmatrix}1\\0\\0\end{bmatrix}e^{i(p_\pm+q)z}\ , \tag{37}$$

where $p_\pm$ is given by (36). For Δ small and $q\lesssim 2$, one of the two waves dominates, and the solution is approximately circularly polarized.

We note that these solutions are azimuthally symmetric in the sense that the only nonvanishing components E_{nm} have $m-n=0$.

C. Conventions

To facilitate the discussion of scattering in the next section, we introduce an inner product

$$\langle \vec{E}' \mid \vec{E} \rangle = \frac{1}{(2\pi)^3} \int \vec{E}'^* \cdot \overleftrightarrow{\epsilon} \vec{E} d^3r , \tag{38}$$

assuming the cholesteric to extend indefinitely. With respect to this inner product the operator

$$L = \overleftrightarrow{\epsilon}^{-1} \vec{\nabla} \times \vec{\nabla} \times \tag{39}$$

is Hermitian. The eigenfunctions of L are the solutions we have constructed to Eq. (1), with eigenvalues ω^2/c^2. Let us normalize these eigenfunctions to δ functions, i.e.,

$$\langle E^{A'}(k',\varphi',p') \mid E^{A}(k,\varphi,p) \rangle = \delta_{A'A} \delta^3(\vec{k}' - \vec{k}) , \tag{40}$$

where $\vec{k}$ has cylindrical coordinates (k,φ,p) and the superscript $A = 1,2$ identifies one of two modes at (k,φ). In terms of components, the normalization condition is

$$1 = \sum_n [\, \epsilon_0 (\, |E_{n1}|^2 + |E_{n,-1}|^2) + \epsilon_z |E_{n0}|^2 + 2\Delta E_{n+2,1} E_{n,-1}] . \tag{41}$$

We specify more exactly the two modes we will use to describe near-forward scattering. Choose $p_\pm$ to have that sign which gives a positive group velocity in the z direction. Let $\vec{E}^{(1)}(0)$ be that $k = 0$ solution which belongs to p_- (and is predominantly E_+), and let $\vec{E}^{(2)}(0)$ be that $k = 0$ solution which belongs to p_+ (and is predominantly E_-). Let the predominant components, $E^{(1)}_{11}(0)$ and $E^{(2)}_{-1,-1}(0)$, be chosen as real and positive. Now define $\vec{E}^{(1)}(k)$ and $\vec{E}^{(2)}(k)$ by continuity in (k,q) along any path in k-q space which does not cross the primary reflection band, keeping $E^{(1)}_{11}(k)$ and $E^{(2)}_{-1,-1}(k)$ real. These choices fully specify the constants E_{nm} in the normalized solutions $\vec{E}^{(1)}$ and $\vec{E}^{(2)}$ for fixed q, ϵ_0, ϵ_z, Δ, and ω.

II. LIGHT SCATTERING

A. General theory

Light propagation in cholesterics is sometimes described as a succession of scatterings or reflections.[10] In this picture the unperturbed solution is a plane wave and the actual modes are described perturbatively. This is not the sense in which we use the words scattering or perturbation theory, as we have included all these effects nonperturbatively. Rather we take the exact modes for the planar texture as the basis of a perturbation theory. A perturbation theory of light scattering in cholesterics which starts from the foregoing solutions as unperturbed solutions takes the effect of the medium exactly into account. We will use these solutions to describe scattering from dielectric fluctuations in Born approximation.

If the dielectric tensor $\overleftrightarrow{\epsilon}$ is replaced by $\overleftrightarrow{\epsilon} + \delta\overleftrightarrow{\epsilon}$, Eq. (1) becomes

$$\overleftrightarrow{\epsilon}^{-1} \vec{\nabla} \times (\vec{\nabla} \times \vec{E}) - \frac{\omega^2}{c^2} \vec{E} = \overleftrightarrow{\epsilon}^{-1} \delta\overleftrightarrow{\epsilon} \vec{E} . \tag{42}$$

The operator on the left is of the form $L - \lambda$. The spectral representation for its Green's function is[11]

$$G^{(\lambda)}_{mm'}(\vec{R},\vec{R}') = \frac{1}{(2\pi)^3} \sum_A \int d^3k \frac{E^A_m(k,\varphi,p;\underline{R}) D^{A*}_{m'}(k,\varphi,p;\vec{R}')}{\omega_A^2/c^2 - \lambda} , \tag{43}$$

where $\omega_A(k,p)$ satisfies the dispersion relation and $\vec{D}^A = \overleftrightarrow{\epsilon}\vec{E}^A$. For large $|\vec{R}|$ we can evaluate $G(\vec{R},\vec{R}')$ by the method of stationary phase.[12] Let $\vec{R}$ have cylindrical components (r,θ,z). Then we find

$$G^{(\lambda)}_{mm'}(\vec{R},\vec{R}') = \sum_A M_A^{-1} E^A_m(k_0,\theta,p_0;\vec{R}) D^{A*}_{m'}(k_0,\theta,p_0;\vec{R}') , \tag{44}$$

where

$$M_A = 4\pi \left| \frac{\partial \omega_A^2}{\partial k^2} \right| \left| k_0 \left[\frac{\partial^2 k}{\partial p^2} \right]_\lambda \right|^{1/2} r . \tag{45}$$

The derivatives are evaluated at (k_0,θ,p_0) on the surface $\omega_A^2(k,p) = \lambda c^2$. The parameters p_0 and k_0 are determined by the requirement

$$\left[\frac{\partial k}{\partial p} \right]_\lambda = -\frac{z}{r} . \tag{46}$$

Geometrically this means that we are at that point on the surface $\omega_A^2(k,p) = \lambda c^2$ at which the normal points in the direction $\vec{R}$.

Using the Green's function $G^{(\lambda)}$ with $\lambda = \omega^2/c^2$ in Eq. (42), we can immediately write down the Born approximation to the scattered field $E_s(R)$ for any incident field E_i. The result is

$$\vec{E}_S(\vec{R}) = \sum_A \vec{E}^A(k_0,\theta p_0;\vec{R}) M_A^{-1} \times \int \vec{E}^{A*}(k_0,\theta,p_0;\vec{R}') \cdot \delta\overleftrightarrow{\epsilon} \vec{E}_i(\vec{R}') d^3R' , \tag{47}$$

in close analogy with the Born approximation in isotropic media. One could also, of course, iterate this solution to obtain higher-order contributions to scattering.

The Born approximation for the scattered field involves the S matrix

$$S_{AA'}=\int \vec{E}^{A*}(k_0,\theta,p_0;\vec{R}')\cdot\delta\epsilon(\vec{R}') \times E^{A'}(k,\varphi,p;\vec{R}')d^3R' . \quad (48)$$

[Here $S_{AA'}$ has nothing to do with the S_n of Eq. (19).] The dielectric perturbation can be represented as a Fourier-Bessel transform,[13] where J_N is the Bessel function,

$$\delta\epsilon_{mm'}(r,\theta,z)=\frac{1}{4\pi^2}\int\sum_N i^N F_{Nmm'}(K,P)J_N(Kr) \times e^{iN\theta}e^{iPz}K\,dK\,dP . \quad (49)$$

Putting this representation for $\delta\epsilon$ into Eq. (48) for the S matrix, we have

$$S_{AA'}=\sum_{\substack{nm\\n'm'N}} E^{A*}_{nm}(k_0)E^{A}_{n'm'}(k) \times F_{Nmm'}(K,p_A-p_{A'}+(n-n')q) \times e^{iN\theta}e^{iPz}K\,dK\,dP . \quad (50)$$

where

$$K=\left[k_0^2+k^2-2kk_0\cos(\theta-\varphi)\right]^{1/2}, \qquad \psi=\tan^{-1}\left[\frac{k\sin\varphi-k_0\sin\theta}{k\cos\varphi-k_0\cos\theta}\right], \quad (51)$$

Here K and ψ are just the polar coordinates of the momentum transfer, projected into the plane perpendicular to the helix axis, as shown in Fig. 1. In particular, if $k=0$ (normal incidence), then $K=k_0$, and $\psi=\theta$.

If the incident field is

$$\vec{E}_i=\sum_{A'} a_{A'}\vec{E}^{A'}(k) , \quad (52)$$

and through the use of compensators, polarizers, etc., we project from the scattered field the linear combination

$$\vec{E}_S=\sum_A b_A\vec{E}^A(k_0) , \quad (53)$$

then the field we observe in the direction (k_0,θ) has amplitude

$$A(k_0,\theta)=\sum_{A,A'} M_A^{-1}b_A S_{AA'}a_{A'} , \quad (54)$$

and the intensity is just

$$I(k_0,\theta)=|A|^2 . \quad (55)$$

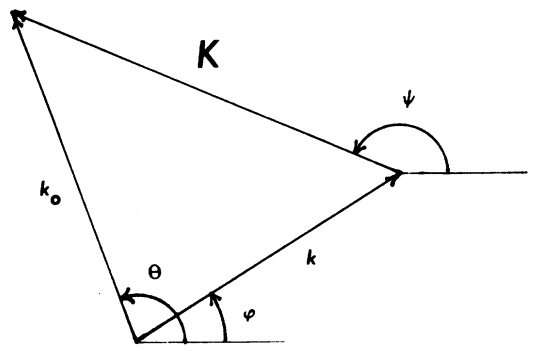

FIG. 1. Relationship of K and ψ, two parameters in Eq. (50) for the S matrix, to initial and final wave vectors.

Equations (49), (50), and (52)–(55) form a natural starting point for any discussion of light scattering in cholesterics.

In the calculations described below, the cholesteric was assumed to be sandwiched between dielectric boundaries perpendicular to the helix axis, with dielectric constant ϵ_0. Linearly polarized light incident from the dielectric is partially transmitted at the boundary, and the transmitted wave becomes the incident wave for scattering. The scattered wave is then partially transmitted at the next boundary and reaches the analyzer. In fact, these corrections for transmission factors were small because of the assumed approximate index matching. The effect of finite sample size was ignored.

B. Example: Order-parameter fluctuations

To illustrate the general theory, let us consider scattering of a beam initially along the helix axis ($k=0$) by fluctuations in the cholesteric order parameter (analogous to fluctuations in layer spacing in a smectic). Theory predicts hydrodynamic fluctuations of this type,[14] and static defects should contain such fluctuations "frozen in." To be specific, consider the replacement

$$qz\rightarrow qz+\delta(\vec{r}) \quad (56)$$

in Eq. (3). Then the only nonzero components of $\delta\vec{\epsilon}$ in Eq. (49) are

$$F_{0,1,-1}(K,P)=2i\Delta f(K,P-2q) , \qquad F_{0,-1,1}(K,P)=-2i\Delta f(K,P+2q) , \quad (57)$$

where $f(K,P)$ is the structure factor, peaked near $K=0$, $P=0$, if the fluctuation is slowly varying.

Equation (50) for the S matrix then becomes

$$S_{AA'}(k,\theta,q)=2i\Delta\sum_{Nnm} mE^{A*}_{nm}(k)E^{A'}_{-m,-m}(0)f(k,p_A-p_{A'}+(n-m)q)e^{i(n-m)\theta}\ . \tag{58}$$

We used Eqs. (54), (55), and (58) to compute the scattered intensity $I(k,\theta)$ for various cholesteric parameters. The results are in some ways contrary to intuition. In particular, there may be considerable structure in the scattered intensity even if the structure factor of the scatterer, $f(K,P)$ is trivial. The scattered intensity may depend nontrivially on the azimuthal angle θ even if the incident beam and the scatterer itself do not depend on θ. This is possible because of the asymmetry of the medium and the consequent absence of selection rules.

In using Eq. (58) we assumed only that

$$f(K,P)=0 \text{ for } |P|\geq q\ , \tag{59}$$

i.e., that order-parameter fluctuations vary slowly in the z direction. The elements of the S matrix are then

$$\begin{aligned}
S_{11}(k,\theta)&=[E^{(1)}_{11}(k)E^{(1)}_{-1,-1}(0)-E^{(1)}_{-1,-1}(k)E^{(1)}_{11}(0)]f(k,p_1-p'_1)\ ,\\
S_{12}(k,\theta)&=[E^{(1)}_{31}(k)E^{(2)}_{-1,-1}(0)-E^{(1)}_{1,-1}(k)E^{(2)}_{11}(0)]e^{2i\theta}f(k,p_1-p'_2+2q)\ ,\\
S_{21}(k,\theta)&=[E^{(2)}_{-1,1}(k)E^{(1)}_{-1,-1}(0)-E^{(2)}_{-3,-1}(k)E^{(1)}_{11}(0)]e^{-2i\theta}f(k,p_2-p'_1-2q)\ ,\\
S_{22}(k,\theta)&=[E^{(2)}_{11}(k)E^{(2)}_{-1,-1}(0)-E^{(2)}_{-1,-1}(k)E^{(2)}_{11}(0)]f(k,p_2-p'_2)\ ,
\end{aligned} \tag{60}$$

where we have used the conventions set up at the end of Sec. I. It is noteworthy that

$$S_{ij}\to 0 \text{ as } k\to 0\ .$$

All S_{ij} are of order k^2 for small k, and there is typically much cancellation between the two contributions to each S_{ij}. This means one must know the fields very accurately to treat scattering moderately accurately. To find S_{ij} accurate to 1 part in 10^3 we solved the dispersion relation for $p(k)$ to 1 part in 10^7. It is a result of the computation that $\vec{E}_3$ and $\vec{E}_{-3}$ contribute as importantly to scattering as $\vec{E}_1$ and $\vec{E}_{-1}$, despite their being very much smaller components. The two-wave approximation[6] omits them altogether, and so is unsuitable for scattering theory.

Note that the θ dependence in the off-diagonal elements of S_{ij} is traceable to the reducible behavior of the exact modes under rotation, and hence, to the asymmetry of the medium.

In Figs. 2–5, we show contours of $I(k,\theta)$ (isophotes) for two values of q (one on either side of the primary reflection) for incident-light polarized vertically (V) and the analyzer either vertical (V) or horizontal (H). We took $f(K,P)$=constant for $|P|<q$, and 0 otherwise. A more realistic structure factor would cut off the scattered intensity at high K.

Figure 6 shows the behavior of the scattering matrix elements S_{ij} for fixed k as a function of q (equivalently ω). The dipolar and quadrupolar patterns of Figs. 2–5 are indicated in Fig. 6 by the large off-diagonal components for q well away from the primary reflection band at $q=1$. Near the primary reflection there is a kind of anomalous diffraction as S_{11} becomes very large. This anomalous diffraction dominates the scattering over a range of q considerably wider than the reflection band itself, and does not show the rich spatial structure that we see for $q\ll 1$ or $q\gg 1$.

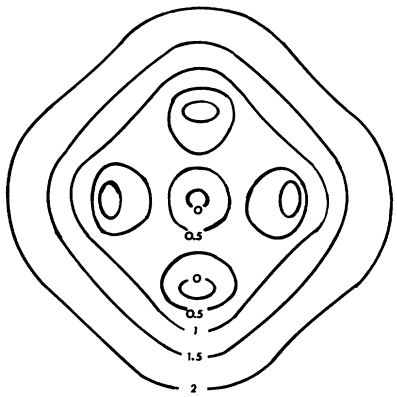

FIG. 2. $\text{Log}_{10}I/I_0$, where I is scattered intensity as it would appear on a screen, and I_0 is an arbitrary constant. The cholesteric parameters were $\epsilon_{||}=2.51$, $\epsilon_{\perp}=2.03$, $\epsilon_z=2.03$, and $q=0.3$, in units where $\epsilon_0\omega^2/c^2=1$. The S matrix was as given in Eq. (60) with $f(K,P)$=constant for $|p|\leq q$, and zero otherwise. Light incident was vertically polarized and along the helix axis. The analyzer was vertical.

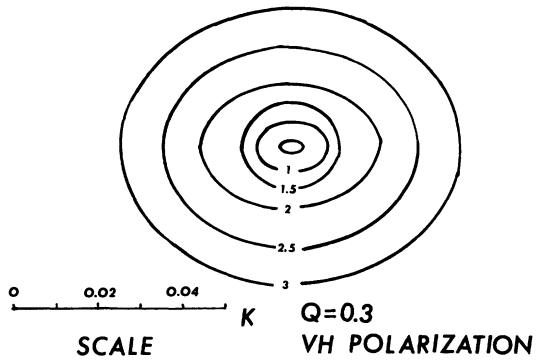

FIG. 3. Like Fig. 2, but with the analyzer horizontal.

We have described results for a material with prolate dielectric tensor. Results with an oblate dielectric tensor are similar. The main difference is a change of sign in the off-diagonal S-matrix elements S_{12} and S_{21}. Thus the typical scattering patterns should be similar to those in Figs. 2—5, but rotated 90°.

The scattering patterns of Figs. 2—5 are qualitatively similar to light scattering patterns observed by Rhodes *et al.*,[15] who first pointed out the wealth of detail and diversity to be seen in light scattering from cholesterics. Their discussion took the light to be a plane wave, so that observed structure in the scattering pattern was ascribed to structure in the scatterer. Of course that is a possibility, but it is also possible that the observed structure arises in the way we have described in this section. We have shown that for scattering from slowly varying

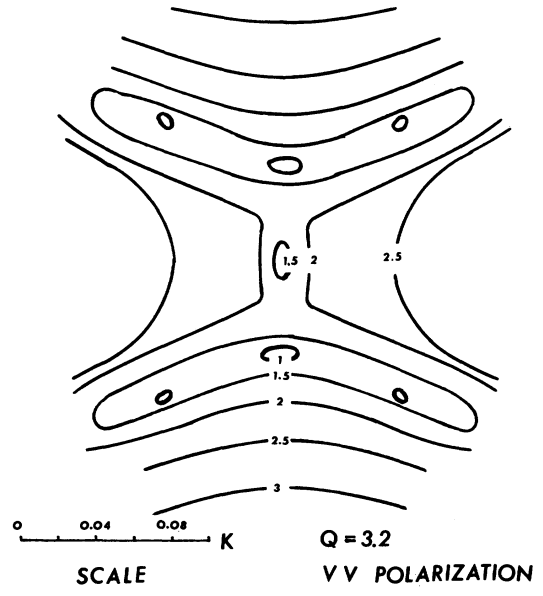

FIG. 4. Like Fig. 2, but $q=3.2$.

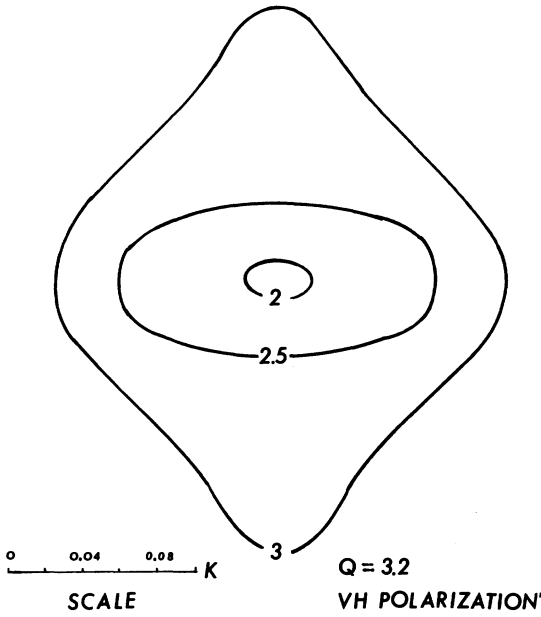

FIG. 5. Like Fig. 2, but with $q=3.2$ and the analyzer horizontal.

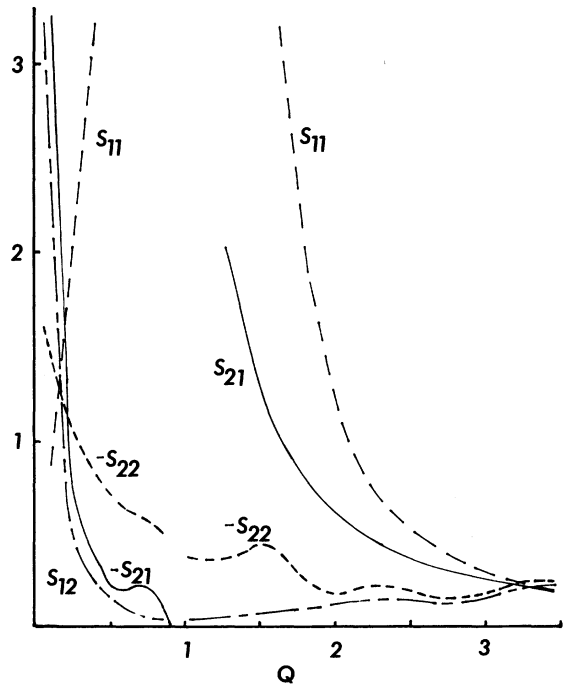

FIG. 6. Behavior of the S-matrix elements S_{ij} for fixed $k=0.1$ as a function of q, in units where $\epsilon_0\omega^2/c^2=1$, according to Eq. (60). The cholesteric parameters were $\epsilon_{||}=2.51$, $\epsilon_{\perp}=2.03$, and $\epsilon_z=2.03$. Units on the ordinate are arbitrary.

order-parameter fluctuations the information encoded in the scattered light is almost entirely information about the medium, and not about the scatterer. Their original observations are intriguing, and it is hoped that the techniques of this paper will aid in clarifying the information that such light scattering patterns contain.

CONCLUSION

We have described the solution to Maxwell's equations for light propagation in a cholesteric planar texture in a form that is convenient for several reasons.

(1) There is a compact algorithm for computing it, which we have given. (2) Behavior of the solution under rotations and reflections is explicit or easily expressed. (3) The S matrix for scattering in Born approximation is easily expressed in terms of this solution.

We have worked out in detail an example of light scattering in cholesterics which shows one may find complex structure in the scattering pattern from even a simple scatterer, because of the complexity of the cholesteric modes.

[1]C. W. Oseen, Trans. Faraday Soc. 29, 883 (1933).
[2]H. de Vries, Acta Crystallogr. 4, 219 (1951).
[3]D. Taupin, J. Phys. (Paris) Colloq. 69, (Suppl.C4), 32 (1969).
[4]D. W. Berreman and T. J. Scheffer, Phys. Rev. Lett. 25, 577 (1970).
[5]R. Dreher and G. Meier, Phys. Rev. A 8, 1616 (1973).
[6]V. A. Belyakov and V. D. Dmitrienko, Fiz. Tverd. Tela (Leningrad) 15, 2724 (1973) [Sov. Phys.—Solid State 15, 1811 (1974)].
[7]V. E. Dmitrienko and V. A. Belyakov, Fiz. Tverd. Tela (Leningrad) 15, 3540 (1973) [Sov. Phys.—Solid State 15, 2365 (1974)].
[8]S. Garoff, R. B. Meyer, and R. Barakat, J.O.S.A. 68, 1217 (1978).
[9]See for example P. G. de Gennes, *The Physics of Liquid Crystals* (Clarendon, Oxford, 1974), Chap. 6, and references therein.
[10]S. Chandrasekhar, *Liquid Crystals* (Cambridge University Press, London, 1977), p. 202ff.
[11]J. Mathews and R. L. Walker, *Mathematical Methods of Physics* (Benjamin, Reading, Mass., 1970), p. 268.
[12]Reference 9, p. 90.
[13]Reference 9, p. 109.
[14]P. C. Martin, O. Parodi, and P. S. Pershan, Phys. Rev. A 6, 2401 (1972).
[15]M. B. Rhodes, R. S. Porter, W. Chu, and R. S. Stein, Mol. Crys. Liq. Cryst. 10, 295 (1970).